

Reliability of COTS MEMS Accelerometer under Shock and Thermomechanical Cycling

Reza Ghaffarian

David G. Sutton, Paul Chaffee, and Nick Marquez

The Aerospace Corporation

Ashok K. Sharma and Alexander Teverovsky (QSS)

NASA Goddard Flight Center

Reza.Ghaffarian@JPL.NASA.Gov, Tel:(818) 354-2059, Fax (818) 393-5245

ABSTRACT

Micro-electro-mechanical sensor systems (MEMS Sensors) are being considered for a variety of applications in space and launch operations. These applications include health and status monitoring, environmental monitoring, automated control, repair and service. A microaccelerometer performance was characterized in detail and their failure mechanisms were identified by subjecting them to 1,000 thermal cycles under extreme temperatures (-65 to 150°C) and to 30,000 shocks at 2,000 g. In addition, several other MEMS sensors (microaccelerometers and temperature sensors) were characterized at the extremes of their temperature ranges. It consists of 10-day test that subjected various microaccelerometers to both continuous thermal cycling between temperatures of -40 °C and +85 °C and mechanical loading. A comparison of the data from microaccelerometers of the same type and between several types will be presented. Self-test output signals and X-ray evaluation test data after completion of 182 thermal cycles will also be presented.

INTRODUCTION

MEMS Definition and Applications

Microelectromechanical systems (MEMS) also known as microsystems technology (MST) or Micromachines are integrated micro devices or systems combining electrical, mechanical, fluidic, optical, (and all physical domains) components fabricated using integrated circuit (IC) compatible batch-processing techniques and range in size from micrometers to millimeters. Miniaturization of mechanical systems promises unique opportunities for new directions in the progress of science and technology. Micromechanical devices and systems are inherently smaller, lighter, faster, and usually more precise than their macroscopic counterparts. However, the development of micromechanical systems requires appropriate fabrication technologies that enable the features such as definition of small geometries, precise dimensional control, design flexibility, interfacing with control electronics, repeatability,

reliability, and high yield and low cost per device will enable the MEMS advanced technologies for the systems in the 21st century.

The majority of today's MEMS products are components or subsystems and their main emphases are on the system levels. Current devices include accelerometers, pressure, chemical, and flow sensors, micromirrors, gyroscopes, fluid pumps, and inkjet print heads. Current MEMS devices for electronic and optical applications include RF MEMS switches, optical network, thermal sensors. Future and emerging applications include high-resolution displays, high-density data storage devices, etc. Current technology mainly addresses millimeter (mm) to micrometer (μm) level MEMS devices. Devices are being further developed in the range of submicron to nanometer scale (nano electromechanical systems, NEMS) for various applications.

Sensors and Accelerometer

Sensors and actuators are the two main categories of MEMS. Sensing systems are used for process control and measurement instrumentation. A transducer is used for both the input and the output blocks of the sensing system. The role of the input transducer is to get information or sense from the real world about the physical or chemical quantity. This is the reason why input transducers are commonly called sensors. Often the electrical signals generated by sensors are weak and have to be amplified or processed in some way. This is done by the signal processing.

For example, accelerometers are widely used for navigational and airbag deployment safety systems in automobiles. The current generation of accelerometer devices integrates electronic circuitry with a micromechanical sensor to provide self-diagnostics and digital output. It is anticipated that the next generation of devices will also incorporate the entire airbag deployment circuitry that decides whether to inflate the airbag. As the technology matures, the airbag crash sensor may be integrated one day with micromachined sensors to form a complete microsystems responsible for driver safety and vehicle stability.

A MEMS solution with lighter weight becomes attractive if it enables a new function, provides significant cost reduction, or both. Space operations will benefit from the comparatively low mass, volume and power required by MEMS. In addition, MEMS are often simple and cheap to produce, install and operate. However, space and launch operations require extremely high reliability and trustworthiness from their systems, especially in human space exploration. MEM devices can often be deployed redundantly to decrease their reliability risk without inflicting large claims on scarce resources. In addition, most microdevices have self-test or diagnostic features as integral capabilities. The task for the systems designer is to use these characteristics (compactness, redundancy, self-test) to enhance the reliability and trustworthiness and extend the lifetimes of MEMS.

Purpose of This Investigation

Packaging and testing of integrated circuit (IC) is well advanced because of the maturity of the IC industry, their wide applications, and availability of industrial infrastructure.^{1,2} This is not true for MEMS with respect to packaging and testing. It is more difficult to adopt standardized MEMS device packaging for wide applications although MEMS use many similar technologies to IC packaging. Packaging of MEMS devices is more complex since in some cases it needs to provide protection from the environment while in some cases allowing access to the environment to measure or affect the desired physical or chemical parameters. The most of the silicon circuitry is sensitive to temperature, moisture, magnetic field, light, and electromagnetic interference. Microscopic mechanical moving parts of MEMS have also their unique issues. Therefore, testing MEMS packages using the same methodologies, as those for electronics packages with standard procedures might not always be possible especially when quality and reliability need to be assessed.

MEMS package reliability depends on package type, i.e. ceramic, plastic, or metal, and reliability of device. The MEMS device reliability depends on its materials and wafer level processes and sealing methods used for environmental protection. Key package reliability issues were reviewed in a previous paper and needs for understanding characterization and understanding failure mechanisms were identified. Implementation of conventional IC reliability to determine if they could accelerate MEMS accelerometer failure was discussed in a recent paper⁴. It was found that while mechanical stresses were more effective in inducing MEMS related failures, some traditional reliability tests did accelerate MEMS-related failure.

This study utilizes conventional environmental test in a synergistic approach to determine reliability issues

associated with commercial-off-the-shelf packages. COTS accelerometers and temperature sensors were considered for evaluation in order to be able to use a large number of them and therefore to generate meaningful statistical reliability data and to determine their associated risk. In addition, it is hoped that comparative performance analysis will identify aberrations or self-test signals that will serve to flag the onset of false readings or device failure. Data of this nature will be invaluable for quality assurance and risk mitigation by formulating the software to assess the veracity of signals from individual sensors and build reliable scenarios from networked systems. This paper will include a large number of test data gathered under thermal and mechanical loading for a variety of MEMS sensors.

ACCELEROMETER TYPES

Table 1 lists types of package that were subjected to environmental characterization. The devices under test included accelerometers manufactured by:

- Motorola Semiconductor Products
- Analog Devices, Inc.,
- Kistler Instrument Corporation

Additionally, temperature measurement devices from Analog Devices and Dallas Semiconductor were tested and used to monitor temperatures within the test chamber. The Analog Device ADXL 250, shown in Table 1 with an asterik mark, was characterized at GSFC under NASA Electronic Parts and Packaging (NEPP)⁵ program. A summary of this characterization also shown below. The other four accelerometers and temperature device characterization were performed by Aerospace Corporation for NASA/Johnson Space Center and also collaborated with JPL under NEPP program⁶. In the following after detail discussion on ADXL 250 and the other four other accelerometers, thermal and mechanical test results for these packages will be presented.

IN-DEPTH CHARACTERIZATION ADXL 250

Package Description

Analog Devices ADXL250 is a dual-axis, surface micromachined accelerometer rated for ± 50 g and packaged in a hermetic 14-lead surface mount Cerpack. The operating temperature range of the part is from -55 °C to $+125$ °C and the storage temperature range is from -65 °C to $+150$ °C. The part can withstand acceleration up to 2000 g.

Table 1 Type and output ranges for accelerometer tested for thermal and mechanical loading and shock

Accelerometer	# of Samples	Output Range	Output sensitivity	Temp. Range Recom by Manufacturer
Motorola XM MAS 40G 10D Micromachined	11	± 4 g	5 mV/g	-40 to 85°C
Motorola MMA1201P Micromachined	5	± 4 g	40 mV/g	-40 to 85°C
Analog Device ADXL05J single Chip	6	± 5 g	400 mV/g	0 to 70°C
Analog Device ADXL 250*	10	± 50 g	40 mV/g	-55 to 125°C
Kistler 830A1 Capacitive	2	± 1 g	1000 mV/g	-20 to 85°C
* Extensive testing on this package performed at GSFC. See Ref 5 All other packages were tested at Aerospace Corp./JPL -40 to 85° C, See Ref 6				

The device is fabricated using a proprietary surface micromachining process that has been in high volume production at Analog Devices, since 1993. The two sensitive axes of the ADXL250 are orthogonal (90°) to each other and in the same plane as the silicon chip. The differential capacitor sensor consists of fixed plates (stationary polysilicon fingers) and moving plates attached to the beam (inertial mass) that shifts in response to the acceleration. Movement of the beam changes the differential capacitance, which is measured by the on-chip circuitry (the clock frequency of the capacitance meter is 1 MHz). Figures 1 provides an overviews of the chip and the capacitive sensor with the close up views of the elements of the sensor including spring attachment and polysilicon finger attachment.

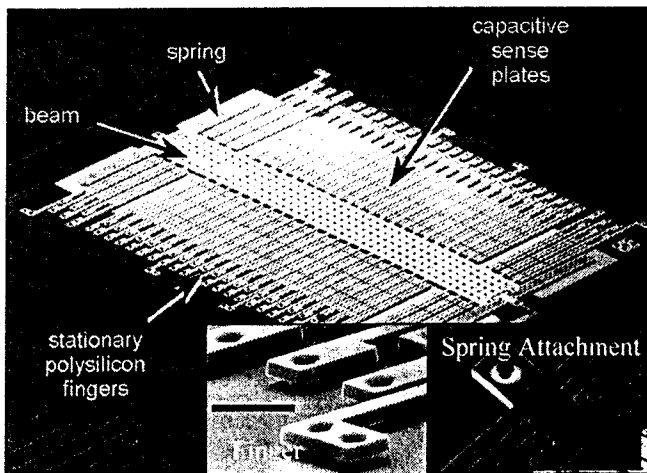


Figure 1 ADXL250 Capacitive Micromachined Accelerometer

Thermal Cycling Characterization

Temperature cycling was performed on 10 parts in the range of -65 °C to +150 °C, with 15 minutes dwell time at each temperature. Measurements were taken after 100, 200, 400, 700, and 1000 cycles. An example of self test outputs with thermal cycling to 1,000 cycles are plotted in Figure 2. No significant changes was observed with thermal cycling. Other electrical parameters showed a similar trend.

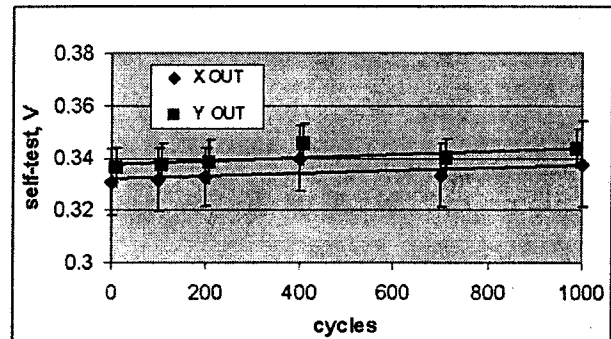


Figure 2 Self-test voltage variation with thermal cycling in the range of -65 to 150°C for ADXL250

Mechanical Shock Behavior

Mechanical shock testing was performed on two groups of devices with ten samples in each group. The first group was subjected to 2000 g shocks in X-direction and the second group to 2000 g shocks in Z direction. Measurements were taken after 100, 300, 1000, 3,000, 10,000, and 30,000 shocks.

Except for one sample of the first group which failed after 10,000 shocks, all other retained their integrity to 30,000

shocks with only minor changes in their parameters (see Figure 3).

All samples, except for the failed one, passed PIND testing. The failed part exhibited permanent noise bursts indicating presence of free particles inside the cavity.

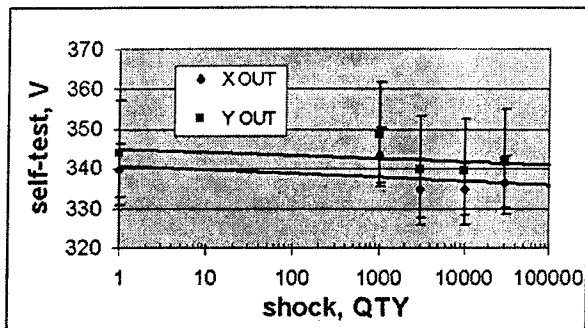


Figure 3 Self-test voltage variation with Thermal shock levels for ADXL250

Failure Analysis

The failed part and several good parts from different groups were decapsulated after testing and examined using optical and SEM microscopes. No microcracks or other defects, which would indicate fatigue-related damage in the sensors, were observed in any of the parts.

A site with a structural anomaly was found in the sealing glass of the failed device. This site had excessive voiding

and porosity, which most likely was due to a contaminant embedded in the glass. Also, Electron beam induced current technique (EBIC) was used in attempt to find any anomaly in the failed Y-channel electronic circuit as compared to the X-channel. EBIC images of the two channels were similar, suggesting that no damage to electronics has occurred.

A small particle with a size of approximately 1 μm , which most likely chipped out from the package, was found jammed between the comb fingers in the Y-channel sensor in the failed part. This particle appears to have wedged electrodes of the capacitor sensor, causing the Y output to be stuck high.

CHARACTERIZATION OF OTHER FOUR ACCELEROMETERS

Four other accelerometers listed in Table 1 were mounted on two boards as shown in Figure 4. The Motorola accelerometers on boards 1 and 2 were mounted in a 16 pin DIP sockets which were wire-wrapped to a 40-pin header socket mounted on each board. The Kistler accelerometer on each board was wired directly to the 40-pin header socket. The Analog accelerometers were packaged in 10-pin TO-100 metal Cans which were inserted into 10 pin sockets and mounted vertically on each board.

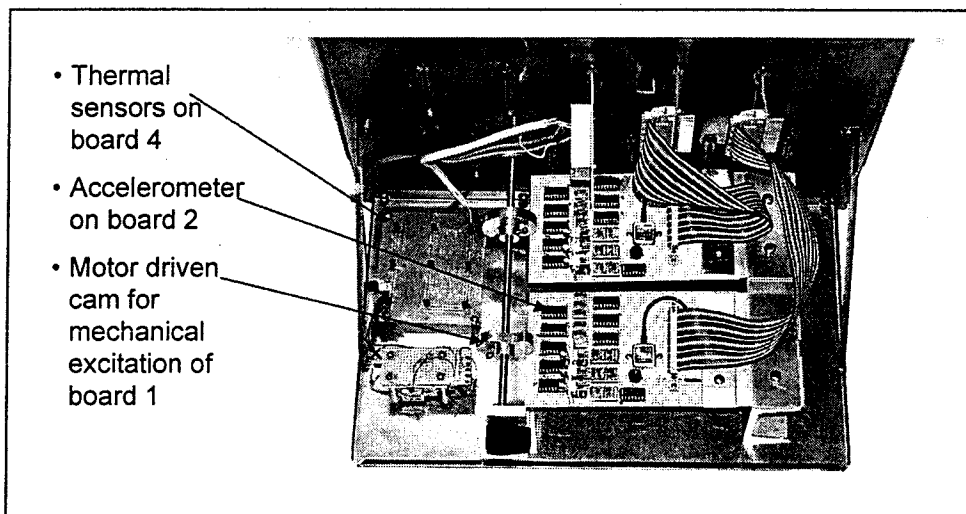


Figure 4 Thermal Cycling experimental test set up with motor driven cam for mechanical excitation

The thermal test was designed to determine the thermal stability characteristics of accelerometers at temperatures of -40 and +85 $^{\circ}\text{C}$. Accelerometers were mounted on fiberglass circuit boards and thermally cycled in a Delta Design Model 9039 environmental test chamber. This chamber has a built-in heater and is chilled using liquid nitrogen (LN_2). The chamber temperature was controlled

with a thermocouple and a Macintosh computer using a LabView program.

Figure 5 shows temperature data for the first two cycles that are recorded at one-minute intervals. The sawtooth pattern was programmed into the test chamber to allow ample time for temperature stabilization and equilibration at the extremes. After an initial ramp up to +85 $^{\circ}\text{C}$ over a period

of 10 minutes, the devices were soaked at that temperature for a period of 20 minutes. The temperature was then ramped down to -40 °C over a twenty minute period and the devices were then held at that temperature for 20-minutes. At the end of that time, the temperature was ramped up for 20 minutes to +85 °C to repeat the cycle. Each full cycle took approximately 80 minutes, divided into four 20-minute segments. This sequence continued for 10 days, 182 cycles.

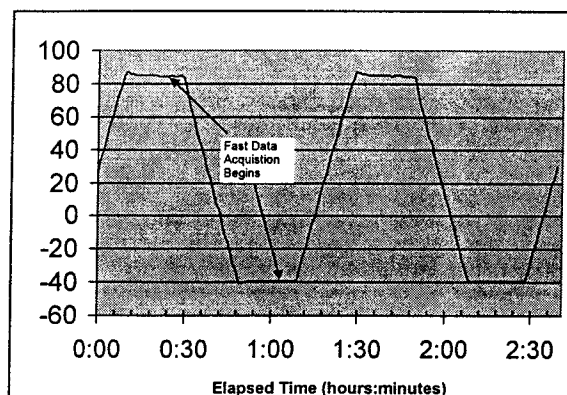


Figure 5 Thermal profile for accelerometers attached on board

Mechanical excitation applied through the free end of fiberglass circuit boards. Boards 1 and 2 were bolted at one end to a short metal extension held in an aluminum block that was in turn bolted to the shelf attached to the door of the test chamber. A motor driven cam mechanism was used to periodically displace the opposite, free ends of these two boards approximately 3/4 inches in the vertical direction and then released them to freely vibrate. Upon release, the resulting board motion was that of a damped vibration of a cantilevered beam which yields alternating accelerations in the vertical direction.

The devices mounted on each of the two boards recorded these accelerations. Boards 1 and 2 were excited to motion once approximately 15 minutes into each temperature soak on every thermal cycle. The two other boards were attached directly to a shelf on the oven door and were not mechanically manipulated.

The outputs of the devices were recorded using a National Instruments AT-MIO-64F-5 data acquisition board and LabView software under Windows NT operating on a personal computer (PC) using a Pentium microprocessor. The data were stored in files on the hard drive of the computer.

Test Results

Figure 6 shows data from three different microaccelerometers recorded during the same oscillation event triggered on cycle 1 at 85 °C. Due to differences in the individual sensors the three curves appear to be different, but they have faithfully recorded similar accelerations. The Motorola XMMAS40 sensor is eight times less sensitive than the Analog Devices ADXL05J, so

on this scale the response is proportionately less. In addition, the ADXL05J appears to be out of phase with the other two sensors. The signal from the ADXL05J is inverted relative to the other two devices due to its opposite orientation on the board.

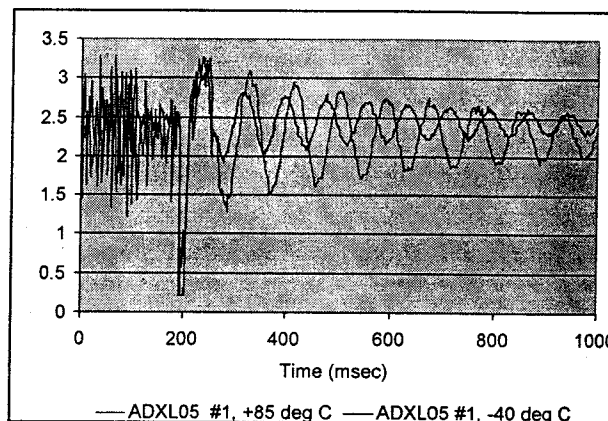
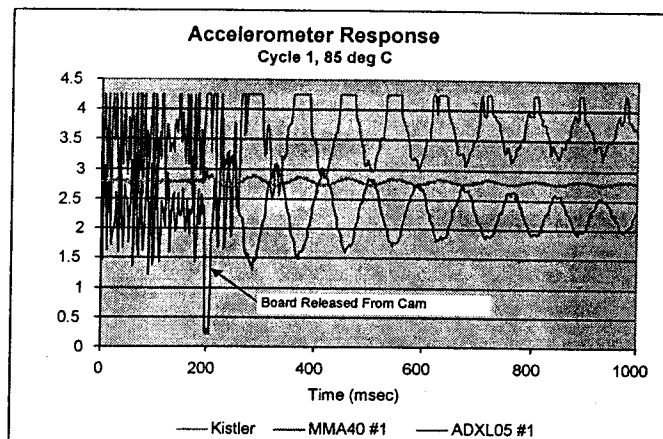


Figure 7 Responses at temperature extremes for ADXL05 Accelerometer at cycle 1

Figure 7 shows the response of the Analog Devices ADXL05J microaccelerometer to two successive events; namely the 85 °C and the -40 °C extremes of cycle 1. There is a delay between these two events of 40 minutes, while the temperature drops. The data at 85 °C is the same as that shown for ADXL05J #1 in Figure 1.

A comparison of the two curves in Figure 7 shows behavior that can be explained by the effects of temperature variations on the aluminum hinge used to mount the board. The peak amplitudes in the acceleration are smaller and the frequency is slightly higher in the event at -40 °C when compared to the one at 85 °C. The frequency of an oscillating cantilevered beam is expected to increase as the square root of the bending modulus. Thus, if the modulus increases as the temperature is reduced, we would expect an increase in the frequency. This is the case for aluminum. The mechanics of our test boards are more complicated, because they are effectively compound beams of thin

aluminum joined to a thick fiberglass test board. However, we expect the temperature trend to be the same and indeed observe a higher frequency at the lower temperature for every case examined.

During continuous monitoring, local peaks were observed in the acceleration on the 2nd and 17th cycles and there were noticeable minima occurring simultaneously on all three sensors at cycles at 82, 110 and 121. These features and near identical occurrences of many smaller features thought to be real due to device failures. Close examination of the individual acceleration records of these anomalies as discussed below revealed that they were anomaly.

Figure 8 shows the first 500 msec of the accelerations sensed by the three ADXL05J sensors during the low temperature portion of cycle 82. It is noticeable that all three devices with peak anomaly registering the same accelerations. This is the first evidence that the unusually low peak values represents real data and not a device failure. Comparison of the responses indicates that cycle 82 was subject to a software dropout resulting in a half-second delay between activation of the cam and the onset of data acquisition. Thus when rapid data acquisition was initiated the oscillations of the board had largely died out, resulting in recorded acceleration peaks comparably smaller than previous cycles.

Being able to distinguish between false signals and real anomalies using the criterion of concurrence from redundant systems is one real advantages that MEMS offers, since the cost of redundancy in terms of mass, power, volume and complexity is minimal.

In addition to acceleration signals, the Analog Devices and Motorola sensors have self test procedures that report a voltage shift if failures are detected. These signals were monitored and recorded for each device during the soak period at the temperature extremes. Figure 9 shows a record of the self-test signals from one of each type of accelerometer for the first two days of the ten days test. According to the manufacturers the self-test signals should be approximately 4 g for the Analog Devices units and 25 g for the Motorola devices. From the table of specifications given earlier these levels correspond to 3.1 V for the ADXL05J, 3.5 V for the MMA1201P, and 2.5 V for the XMMAS40. The actual signals vary somewhat from these specifications, but they are remarkably stable over the entire 10 day period. The data shown are entirely representative of the entire record including the cycles where the low peaks were recorded.

The only remarkable thing about these signals is the repetitious variation with temperature. The ADXL05J self-test signal is higher at the low temperature extreme and lower at the highest temperature. Both Motorola accelerometers exhibit the opposite behavior. The range of

measured voltages from all the sensors is within the parameters specified by the manufacturers for properly functioning accelerometers. This is further evidence that the low peak values are not due to faulty signals.

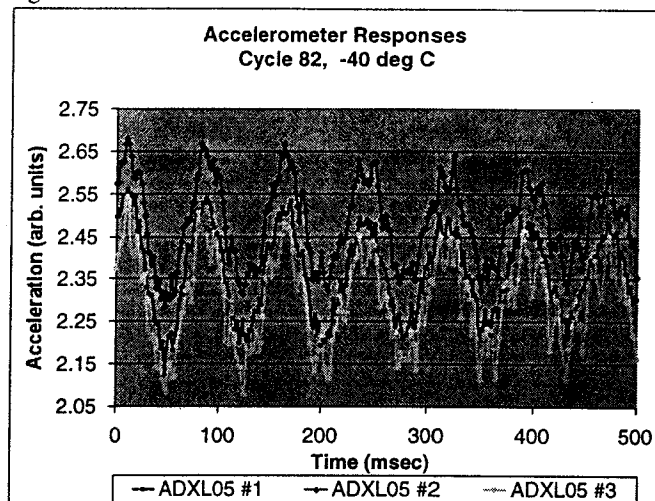


Figure 8 Accelerometer responses at 82 cycles (-40/85°C)

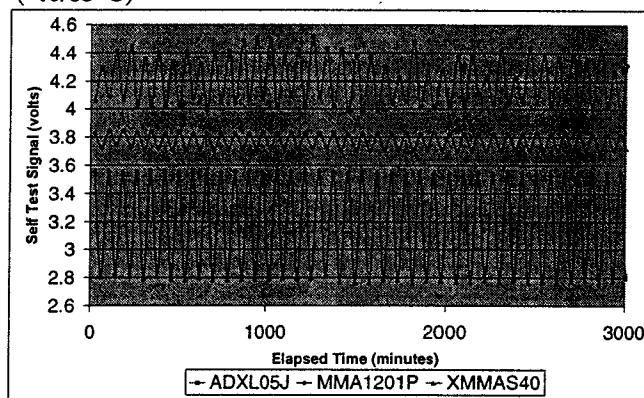


Figure 9 Self test results with exposure thermal cycle time

NON DESTRUCTIVE CHARACTERIZATION BY X-RAY

Non-destructive evaluation using a real time X-ray was performed prior to and after about 182 thermal cycles to assure quality of package. X-ray photos for accelerometers are shown in Figures 11 to 13. No failure or particulates that may represent gross failure was observed. After establishing such baseline, these accelerometer will be further subject to thermomechanical exposure till failure.

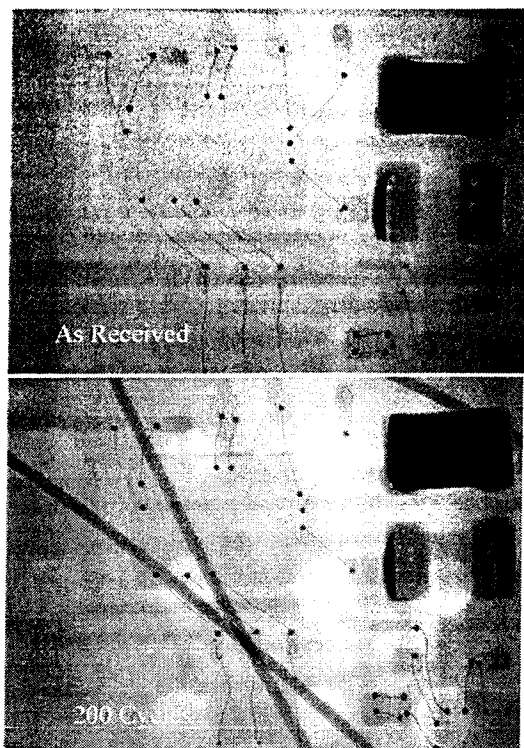


Figure 11 As Receive and after 200 cycles of Kistler Accelerometer



Figure 12 As Receive and after 200 cycles of MMA1201 Accelerometer

CONCLUSIONS

- Analog devices ADXL250 successfully passed 1,000 thermal cycles in the range of -65°C to 150°C as well as 30,000 mechanical shocks of 2000 g in the Z direction and 10,000 shock in the X direction with minor parametric changes

- Four accelerometers; Motorola XMMAS40G, MMA1201P, Analog devices ADXL05J, Kistler 8303A1; and a temperature sensor performed within their nominal specification showing no degradation verified by electrical and non-destructive evaluation when subjected to 182 cycles in the range of -40°C to 85°C . This temperature regime was higher than operating temperatures of ADXL05J and 8303A1 accelerometers.

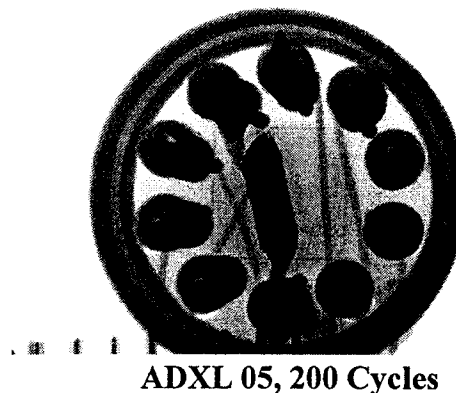


Figure 13 ADXL05 accelerometer after 200 cycles

ACKNOWLEDGEMENT

Portion the research described in this publication was carried out by the Jet Propulsion Laboratory, California Institute of Technology, under a contract with the National Aeronautics and Space Administration.

REFERENCES

1. Ghaffarian, R. "Chip Scale Packaging Guidelines," Interconnection Technology Research Institute (ITRI), Jan. 2000, <http://www.ITRI.org>
2. Ghaffarian, R., "Ball Grid Array Packaging Guidelines," Interconnect Technology Research Institute (ITRI), August 1998,
3. Ghaffarian, R., Ramesham, R. "Comparison of IC and MEMS Packaging Reliability Approaches," Surface Mount Technology Association, Chicago, 2000
4. Delak, K.M., et al., "Analysis of Manufacturing Scale MEMS Reliability Testing," MEMS Reliability for Critical and Space Applications, SPIE Volume 3880, Santa Clara, Sept. 1999
5. Sharma, A., Teverovksy, "Evaluation of thermo-mechanical Stability of COTS Dual-Axis MEMS Accelerometers for Space Applications," COTS MEMS Conf., Knowledge Foundation, Berkley, August, 2000
6. Sutton, D.G., et al., "Reliability Risk Assessment of COTS MEMS Accelerometer Under Thermomechanical Cycling," Aerospace Corporation Report No. TOR-200(2124)-2